Engineering 59 (2026) 158–167

Contents lists available at ScienceDirect

Engineering

journal homepage: www.elsevier.com/locate/eng

Research
Low Carbon Transformation for Conventional Energies—Article

# The Staged, Pressurized Oxy-Combustion Technology: Status and Application to Boiler Retrofits to Yield Carbon-Negative Power via Biomass

Duarte Magalhaes, Mao Cheng, Zachariah Wargel, Richard L. Axelbaum *

*Department of Energy, Environmental and Chemical Engineering, Washington University in St. Louis, St. Louis, MO 63130, USA*

ARTICLE INFO

*Article history:*
Received 1 April 2025
Revised 22 September 2025
Accepted 24 November 2025
Available online 26 November 2025

*Keywords:*
Staged pressurized oxy-combustion
Carbon negative power
Cogeneration
Industrial decarbonization
Carbon capture and storage

ABSTRACT

Recognizing the benefits of pressurization and fuel staging on the efficiency of oxy-combustion, the staged, pressurized oxy-combustion (SPOC) process was introduced in 2012. The combination of fuel staging and pressurized oxy-combustion results in a more compact plant, a higher plant efficiency and reduced costs for pollutant and greenhouse gas removal compared with plants equipped with conventional carbon capture. This approach to power generation enables a modular boiler design and optimizes the plant for flexible operation, which is essential to meet the demands of the modern grid when it contains intermittent power sources. Originally designed to burn coal, the SPOC process is well-suited for biomass because the combustion of biomass leads to a high moisture content in the flue gas and the SPOC process is able to recover the latent heat of this moisture, enhancing system performance over that of traditional biomass combustion at atmospheric pressure. The present work is focused on evaluating the potential for utilizing the SPOC process in retrofit applications wherein the boilers of an existing plant are replaced with the SPOC process, and woody biomass is used as the fuel to yield carbon-negative power. Two applications are considered: power generation and cogeneration (heat and power). Modeling these systems in Aspen Plus demonstrates that the SPOC process surpasses the performance of baseline plants with post-combustion capture (PCC) for both power generation and cogeneration. Specifically, compared to a PCC equipped plant, the SPOC power plant has 33% higher efficiency, and the SPOC cogeneration plant reaches 42% higher net energy. Experimentally, the existing SPOC facility was fired for the first time with 100% biomass and after minor improvements were made to the feeding system, the facility demonstrated excellent performance during startup, steady-state operation and turndown.

## 1. Introduction

The rapid rise of data centers, electric vehicles (EVs) and electrification has increased the demand for reliable, flexible, low-cost, and low-carbon or carbon-negative power. Electricity consumption in data centers, which represented 4.4% of the total usage in the United States in 2023, is expected to rise sharply and reach ~9% of US electricity consumption as early as 2028, based on a moderate future scenario by the Lawrence Berkeley National Laboratory [1]. Tech companies are deeply invested in the artificial intelligence (AI) race and thus have a strong need to build data centers. In fact, Amazon, Meta, Microsoft, and Alphabet are expected to spend a combined 320 billion USD in 2025 to build AI infrastructure. Since these same companies have strong climate commitments, the power to feed these data centers needs to be not only reliable and low-cost, but also come from sources that are low-carbon or, ideally, carbon-negative.

Carbon capture and storage (CCS) technologies have the potential to offer reliable 24/7 carbon-neutral or carbon-negative power, and they may also be compatible with a retrofit to an existing plant, which makes them attractive for repurposing baseload thermal plants. The most common retrofit technology is post-combustion capture (PCC) which involves absorption/desorption of $CO_2$ using amine-based solvents. While PCC has been commercially applied to coal-fired power plants, it requires a high thermal

---

* Corresponding author.
*E-mail address:* axelbaum@wustl.edu (R.L. Axelbaum).

https://doi.org/10.1016/j.eng.2025.11.016
2095-8099/

energy for solvent regeneration, resulting in an efficiency penalty of 10–11 percentage points. Moreover, solvent degradation is a challenge and not well understood, especially for biomass where feedstock variability exacerbates the challenge of degradation.

In first-generation oxy-combustion, which is operated at atmospheric pressure, the feedstock reacts with oxygen supplied from an air separation unit (ASU). The oxygen is diluted with recycled flue gas to control flame temperature and heat flux in the boiler. In this process, the efficiency loss, which can be as high as 7–8 percentage points, is primarily due to parasitic loads associated with the ASU, the $CO_2$ processing unit (CPU), and the recirculation of a significant portion of the flue gas (approximately 70%) [2].

Pressurized oxy-combustion (POC) can help mitigate some of the drawbacks of first-generation oxy-combustion, offering key advantages that increase the process efficiency and reduce capital costs. One of the key advantages is the ability to condense the moisture in the flue gas at a temperature that is sufficiently high that this energy can be integrated into the steam cycle (latent heat recovery), resulting in an efficiency gain of up to 2.5 percentage points [3]. Furthermore, the simultaneous removal of $SO_x$ and $NO_x$ in a single pressurized column significantly reduces both capital and operational costs compared to conventional flue gas desulfurization (FGD) and selective catalytic reduction (SCR) systems, respectively.

To further enhance efficiency, reduce costs, and increase the flexibility of POC systems, Washington University in St. Louis (WashU) introduced the concept of fuel staging to minimize flue gas recycle (FGR), and applied this strategy to POC, leading to the development of the staged, POC (SPOC) process [4]. The modular SPOC process features a plant design that combines fuel staging with POC, resulting in a more compact plant size, higher efficiency, improved operational flexibility and reduced costs for pollutant removal and carbon capture. Additionally, the small modular boilers and pollutant removal units are factory fabricated off-site, further reducing capital costs.

Washington University, with guidance from industry leaders, has commissioned a single-stage 100 kW thermal ($kW_{th}$) pressurized oxy-combustor as well as a direct contact cooler (DCC) capable of treating flue gas. Extensive experimental testing, combined with computational fluid dynamics (CFD) modeling using Reynolds Averaged Navier-Stokes (RANS) and Large Eddy Simulation (LES), has led to improved combustor performance as well as a design for a full-scale 550 megawatt (MW) plant [4–10]. Recently, the authors integrated the pressurized combustor with a boiler and the DCC, and the integrated facility was demonstrated using Powder River Basin (PRB) coal. Cumulatively, the facility has been operated for 8+ years at thermal inputs ranging from 8 to 125 $kW_{th}$ with various solid fuels (primarily coal), for a total of 1500 h. Excellent combustor and DCC performance has been achieved [11–13] for coal firing even with low excess oxygen (< 2 vol%). This includes excellent flame stability, complete burnout and low $NO_x$ and $SO_x$ ($NO_x$ < 50 parts per million by volume (ppmv), $SO_x$ < 10 ppmv at the DCC outlet). It should be noted that oxy-combustion at high-pressure is fundamentally a low-$NO_x$ process [14], resulting in low levels of $NO_x$ (< 200 ppmv) even upstream of the DCC.

Process optimization of the SPOC process via Aspen Plus modeling and techno-economic analysis (TEA) have been performed for power generation. The SPOC power plant has an efficiency of 34.5% (higher heating value (HHV)) when using PRB subbituminous coal, outperforming both the National Energy Technology Laboratory (NETL) atmospheric-pressure oxy-combustion baseline case (S12F) by 3.3 percentage points and the PCC equipped air-fired case (S12B) by 7.5 percentage points for the same steam cycle [15]. Furthermore, according to an independent study performed by Électricité de France, the modular SPOC process has a plant efficiency that is 4.8 percentage points higher than that of ITEA SpA's ISOTHERM process, which is another POC technology [16]. The ISOTHERM process uses a coal–water slurry and considerable flue gas recirculation to attain flameless combustion in a slightly pressurized environment. The process minimizes thermal $NO_x$ and is fuel tolerant, but the high water content in the slurry and the large amount of recirculated flue gas result in significant exergy losses and efficiency penalties as compared to the SPOC process. A comparison of the coal-fired SPOC process with the competing POC technology was conducted by Hu et al. [17] for 600 MW power generation, and it was showed that SPOC can achieve higher efficiency when using the same fuel and steam cycle parameters. Li et al. [8] focused on the evaluation of the SPOC cycle for a 550 MW biomass power generation and found the net thermal efficiency (HHV) of the SPOC process to be 35.2%. These recent studies [8,17] utilized a prior concept of SPOC in which each boiler had a different stoichiometric ratio for the purpose of flame temperature and heat flux control, and focused on large-scale power generation (550–600 MW). However, the current design of the SPOC process opts for identical boilers—thereby avoiding the complexity of having different stoichiometric ratios for each stage and requiring different boiler geometries and a pre-determined number of stages. Accordingly, the process can be tailored to a wide range of net output and number of stages, making it ideal for smaller scale biomass firing and boiler retrofits.

Despite having been initially conceptualized for coal-based power generation, the attributes of the SPOC process make it intrinsically valuable for biomass-based power generation, wherein carbon negative power is produced. Pressurized combustion not only increases residence times but also accelerates oxidation and gasification reaction rates, ensuring excellent burnout even for large biomass particles. Moreover, the high moisture content in the biomass flue gas is not detrimental to system efficiency, as is the case for traditional atmospheric-pressure biomass combustion, because the latent heat can be recovered in the SPOC process, resulting in improved system performance. The present paper addresses two pressing needs in POC research for carbon-negative applications: ① development of a process model to evaluate the SPOC plant performance for both power generation and cogeneration retrofits when using biomass at the 50–60 megawatt electrical ($MW_e$) scale, and ② experimental demonstration of biomass firing under POC conditions at the 100 $kW_{th}$ scale.

## 2. Materials and methods

### 2.1. Integrated POC facility

The POC facility at WashU, commissioned in 2016, is rated at 125 $kW_{th}$ thermal input. The facility is equipped with industry-standard controls and measurement equipment and is fully automated so that it can be operated by a single operator in a control room. The two key pilot-scale prototypes include the pressurized combustor–boiler and the DCC, which are shown in Fig. 1. A simplified flow diagram of the pilot-scale integrated facility is shown in Fig. 2. The oxygen, dilution $CO_2$, and solid fuel are introduced into the combustor using a coaxial low-mixing burner. The combustor-boiler is designed to parallel the full-scale conceptual design and is contained in a 20 ft (1 ft = 0.3048 m) long pressure vessel rated for 20 bar (1 bar = $10^5$ Pa) and with multiple ports for instrumentation and optical access. Since the pressure vessel is cylindrical and radiative heat transfer is augmented under pressure, the low-mixing burner along with the slender combustor design are key to a more uniform heat flux along the length of the combustor. The combustor is designed to yield a temperature at the inlet of the boiler test section that resembles that of the inlet

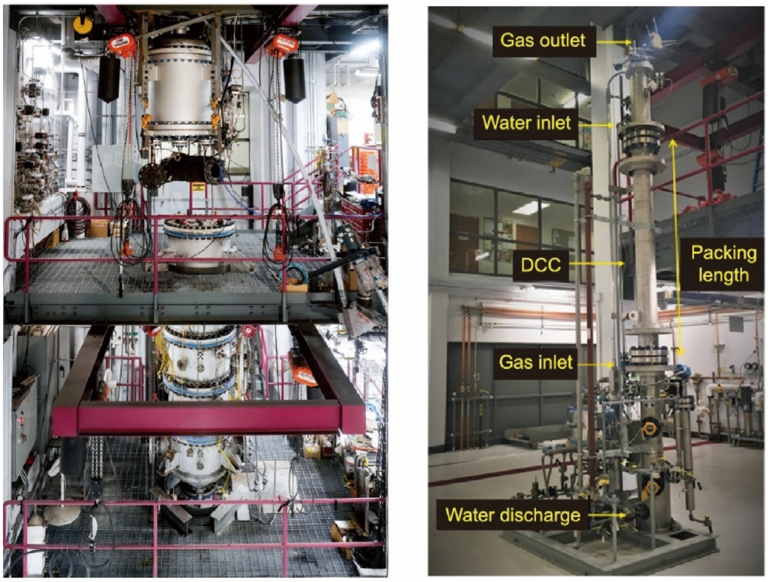

(a) (b)

**Fig. 1.** The SPOC research facility: (a) combustor-boiler and (b) DCC.

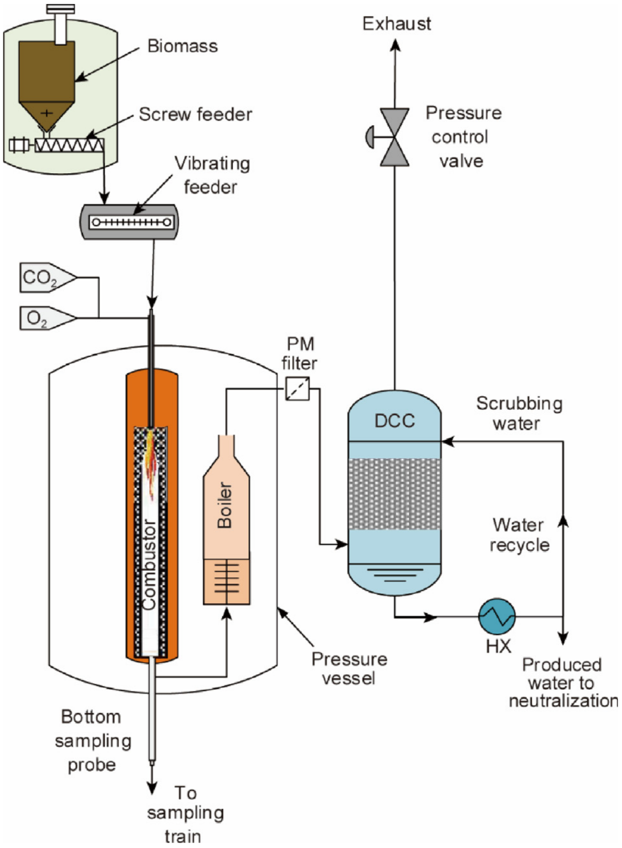

**Fig. 2.** Simplified process flow diagram of the integrated SPOC pilot-scale facility. HX: heat exchanger.

temperature to the superheater in a full-scale system (i.e. below the ash initial deformation temperature). Since the typical flue gas temperature entering the superheater is *circa* 1200 °C and the surface/volume ratio is higher at the pilot scale vs full-scale, this requires the combustor to be refractory lined and insulated to prevent significant heat loss, as opposed to having a typical water-wall boundary. The boiler includes a test section that emulates the fire-side of a SPOC full-scale superheater to allow for experimental validation of heat transfer at high-pressure. The combustor and boiler are connected via a horizontal section that utilizes low-density refractory to minimize heat loss between the combustor outlet and the boiler inlet. An oil-cooled section downstream of the boiler allows the flue gas to be further cool to 340 °C, yielding conditions that emulate the conditions at the outlet of the SPOC Economizer in the full-scale plant. This temperature maintains the heat exchanger surfaces above the acid dew point to prevent corrosion. Upon leaving the boiler, the flue gas is filtered and then enters the DCC. The DCC column has a dual role. First is to cool and condense the moisture from the flue gas, which occurs in the bottom stages. Second is to remove $SO_x$, $NO_x$, and HCl via conversion to dilute sulfuric, nitric, and hydrochloric acids, respectively.

Flame monitoring is accomplished using a Fireye flame scanner, thermocouples, and differential pressure gauges. The state-of-the-art sampling systems include: ① a patented high-pressure high-temperature flow cell coupled to a Malvern Panalytical Insitec for particle size analysis [18], and ② a pressurized Nafion dryer coupled to a Fourier transform infrared (FTIR) analyzer for measuring online flue gas composition. These two devices allow particle and gas measurements to be performed online at high pressure, avoiding the sample bias that would result from depressurization. In the present work, these systems were tested for biomass firing for the first time. The sampling train for gas and particulate sampling used in this study is shown in Fig. 3.

The flue gas is sampled using an isokinetic sampling probe inserted through the bottom of the combustor (upstream of the DCC), while minimizing particle loss due to thermophoresis. The flue gas then flows through a high-pressure, high-temperature filter to collect particulates (ash/char) for further analysis. All lines are heat traced and kept at a controlled temperature to prevent loss of condensable species and sampling bias. Downstream of the filter, the flue gas follows through one of two paths: ① a high-pressure gas cell coupled with an FTIR gas analyzer, and ② an atmospheric-pressure Testo gas analyzer. The flue gas is cooled and dried before entering rotameters for verification of flow rates, ensuring isokinetic sampling conditions.

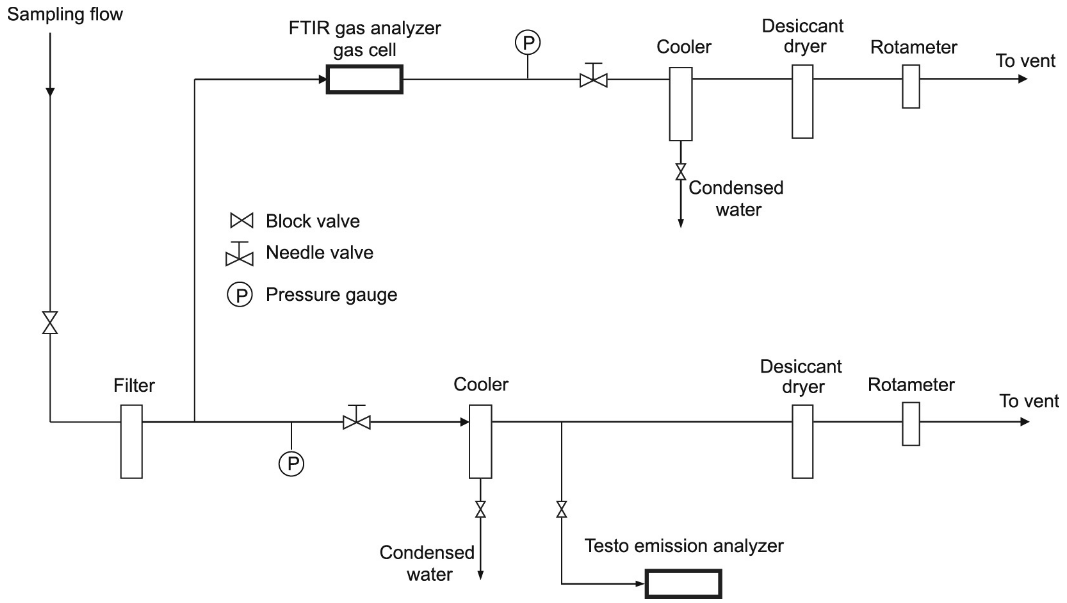

**Fig. 3.** Sampling train used for gas and particulate measurements in the integrated pilot-scale SPOC facility.

### *2.2. Process description and modeling*

A process modeling and performance approach that is similar to that used in the NETL studies was used in this study, and the SPOC process was modeled using Aspen Plus for applications to boiler retrofits in both power generation and cogeneration. The SPOC process for boiler retrofits is assumed to be a subcritical (subC) single reheat cycle (166 bar absolute (bara)/566 °C/566 °C). The boiler island modeled (Fig. 4) includes all major components such as the ASU, lockhoppers, SPOC boilers, high temperature heat recovery (HT-HR), baghouse filter, DCC, and CPU. The steam turbine island also includes all major components such as the high-pressure (HP), intermediate-pressure (IP), and low-pressure (LP) turbines, generator, boiler feed pump turbine, condenser, deaerator, boiler feed pump, and feedwater heaters. Heat integration for the ASU, CPU, DCC (LP heat recovery) and HT-HR was also modeled.

A conceptual process flow diagram for a modular SPOC power plant is shown in Fig. 4. This simplified process flow diagram is applicable to both power generation and cogeneration, with the exception of the condenser/cooling tower, which is absent in the cogeneration plant, as the steam condensate is utilized directly in the production process in cogeneration. Detailed process flow diagrams for both plants are included in Section 3. Oxygen (95.9 mol% purity) is produced via a cryogenic ASU [19–21] and the heat generated from the compression of air is integrated into the steam cycle and utilized for boiler feed water regeneration. Unique to the SPOC process, the boilers are arranged in a series–parallel configuration. This innovation allows for minimizing FGR and enables a modular boiler design. When applied to biomass firing, sustainably-sourced wood waste is fed with a pneumatic dry feeder using a small amount of cold FGR as motive gas, and the amount of feedstock fed to each of the nominally four boiler stages

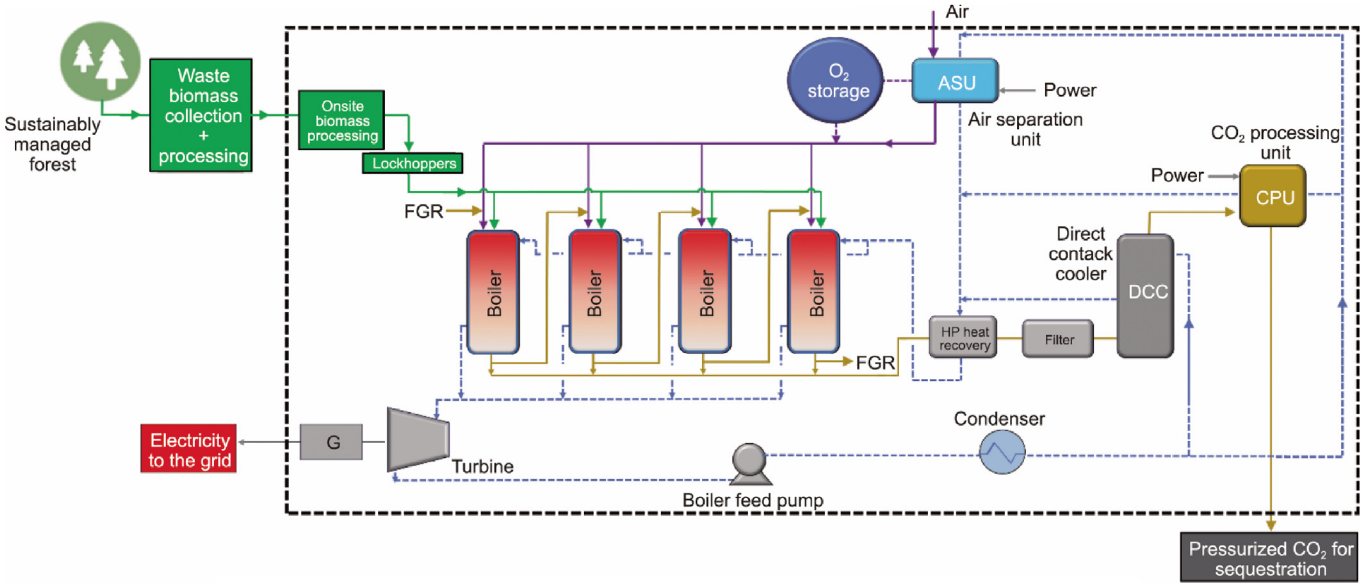

**Fig. 4.** Modular SPOC simplified process flow diagram with indication of the plant boundary.

is nearly the same. Only a small amount of the total flue gas (< 30%) is recycled back to the first boiler stage to dilute the oxygen and control flame temperature in this stage [3]. Then, a portion of the flue gas from the first boiler is fed into the next stage and this flue gas acts as the diluent for the oxygen. The rest is sent downstream. Note that the amount of flue gas sent to the second stage is nearly the same as the recycled flue gas sent to the first stage, so the operations of both boilers are similar, but the total amount of FGR has not changed since the flue gas entering the second stage was not recycled. The process is repeated for the last two boilers such that FGR is only needed for the first stage, thereby leading to improvements in plant efficiency over traditional oxy-combustion power plants. The exit temperature of the flue gas from each combustion stage and economizer is 340 °C.

Downstream of the pressurized boilers, the flue gas stream is fed into a high-pressure heat recovery unit (Fig. 4), where heat is extracted and integrated into the power cycle and the flue gas is cooled to slightly above the acid dew point temperature. Thereafter, fly ash particles in the flue gas are removed by a particulate filter. Subsequently, the flue gas is further cooled in the DCC, and the water leaving the bottom of the DCC is at a sufficiently high temperature that it can be used for boiler feed water heating to around 145 °C without any steam extraction, thus improving efficiency over that of atmospheric-pressure operation.

In this process, the $CO_2$ capture efficiency is 95% or higher. To meet sequestration/pipeline requirements, the flue gas exiting the DCC is purified and compressed in the CPU to remove trace amounts of $N_2$, $O_2$, and Ar (note: $SO_x$, $NO_x$, and HCl are scrubbed in the DCC). Following purification, the ~99 vol% pure $CO_2$ stream is compressed and sent for sequestration/utilization. Importantly, the energy requirement for compression of $CO_2$ is much lower compared to that of a state-of-the-art PCC since the $CO_2$ stream is already at 15 bara. This is a key benefit of SPOC, since the compression of the $O_2$, which allows for pressurized combustion and its subsequent benefits, is offset by the decrease in compression costs for the $CO_2$.

The steam turbine used in the SPOC design is similar to the atmospheric oxy-combustion baseline NETL case, and the isentropic efficiencies of the HP, IP, and LP turbines were taken from Ref. [15]. Importantly, the enhanced heat recovery capability resulting from the capture of latent heat from the moisture in the combustion products eliminates the need for the LP feedwater heater train. In atmospheric pressure systems, this latent heat would be lost up the stack.

The upstream greenhouse gas (GHG) emissions from raw material acquisition and raw material transport were accounted for using NETL Upstream Dashboard Version 3 [22]. The upstream $CO_2$ emissions corresponded to approximately 10% relative to the total emissions generated from the oxy-combustion process within the plant boundary.

## 3. Application to boiler retrofits

### 3.1. Retrofit of an existing plant to generate carbon-negative power

As an example of applying the SPOC process in a retrofit application, a subC (166 bara/566 °C/566 °C) pulverized coal (PC) plant that is presumably slated for retirement is retrofit with the SPOC process and operated with biomass. The process flow diagram is shown in Fig. 5, and a comparison of the thermal efficiency of SPOC vs several baseline power plants is presented in Table 1 [2,23,24]. The goal of the retrofit plant is to yield a net removal of 500 000 tonne $CO_2$ equivalent per year ((t $CO_2$e)$\cdot$a$^{-1}$) by using 100% sustainably-sourced wood waste as the feedstock and with a capture efficiency of 95% (Table 2). This process was modeled using Aspen Plus and is a modification of the performance modeling of the SPOC PC power plant that was performed by the Electric Power Research Institute (EPRI) [15]. A total biomass feed rate of 340 000 t$\cdot$a$^{-1}$ (HHV thermal input of 190.9 megawatt thermal ($MW_{th}$) is used to generate a turbine gross output of 82.6 $MW_e$, and after powering auxiliaries the net output of the plant is 61.2 $MW_e$ (Table 3).

The plant HHV thermal efficiency is 32.1% for the subC steam cycle, which is higher than the average efficiency of the existing coal power plants in the United States, demonstrating that the SPOC plant can reach the existing plant efficiency while removing $CO_2$ from the atmosphere. A comparison of the thermal efficiency for the SPOC process with several NETL baseline cases is presented in Table 1. For the case of a supercritical (SC) steam cycle, the thermal efficiency (HHV) of the SPOC biomass-fired plant reaches 34.9%. This is 7.9 percentage points higher than the NETL sub-bituminous SC air-fired PCC plant (S12B), and 3.9 percentage points higher than the NETL baseline sub-bituminous SC oxy-fired atmospheric plant (S12F). The PCC equipped plant loses efficiency due to the large heat duty in the reboiler required for $CO_2$ desorption. The performance improvement over S12F is a result of the improved heat recovery from the flue gas and from the reduced auxiliary power consumption from the ASU and CPU. Another reduction in auxiliary load is due to the reduced duty of the recycle fan (or induced draft fan) since the volume of gas being recycled in SPOC (< 30%) is substantially lower than in S12F (70%). Moreover, S12F loses efficiency due to air ingress. Notably, the efficiency of the biomass-fired SPOC process is the same as that of coal-fired SPOC, and this is the result of the effectiveness of the heat recovery in the SPOC process. In comparison with S12F (the coal-fired atmospheric oxy-combustion baseline), SPOC is 3.8 percentage points more efficient, and even the subC 100% biomass fired SPOC cycle is 1.1 percentage points more efficient.

The most recent (2023) NETL baseline cases (B12B, PA1, PA2, PA3, and PA100) utilize a more advanced turbine which by itself results in an increase in efficiency of 1.1–1.6 percentage points as compared with prior studies, including the SPOC study, which uses an older turbine. Were the SPOC process equipped with a similar turbine, its HHV efficiency is conservatively estimated to reach 36%. It should be noted that the NETL baselines for biomass energy with CCS (BECCS) (PA1, PA2, PA3, and PA100) utilize green biomass with 50 wt% moisture, which is detrimental to cycle efficiency, while the SPOC cycle utilizes pre-pelletized biomass with 10 wt% moisture. The authors estimate the thermal efficiency of PA100 to be up to 27% if the drier biomass were used (10 wt% moisture). This is significantly higher than the 23.3% reported by NETL, but still 9 percentage points below the efficiency of the SPOC cycle using the same biomass and a similarly advanced turbine. In fact, the efficiency of the SPOC process with a subC steam cycle is 5.1 percentage points higher than the NETL baseline using an SC steam cycle for the same biomass fuel, resulting in an additional 19% more energy generated.

### 3.2. Retrofit of a cogeneration plant to produce carbon-negative heat and power for the recycled paper industry

In the United States, a conventional recycled paperboard mill typically has a large cogeneration plant, burning fossil fuels to supply steam for process heat for the pulping and pulp drying processes, and electricity to the machinery [25]. The manufacturing of recycled paper/paperboard is done in a series of steps: collection of used paperboards, pulping, pulp refining, drainage and pulp pressing, pulp drying, and conversion to the final product. Both the pulping and pulp drying processes require a significant amount of steam. During pulping, steam is directly used to heat the mixture and break down the paper, whereas during drying, steam is

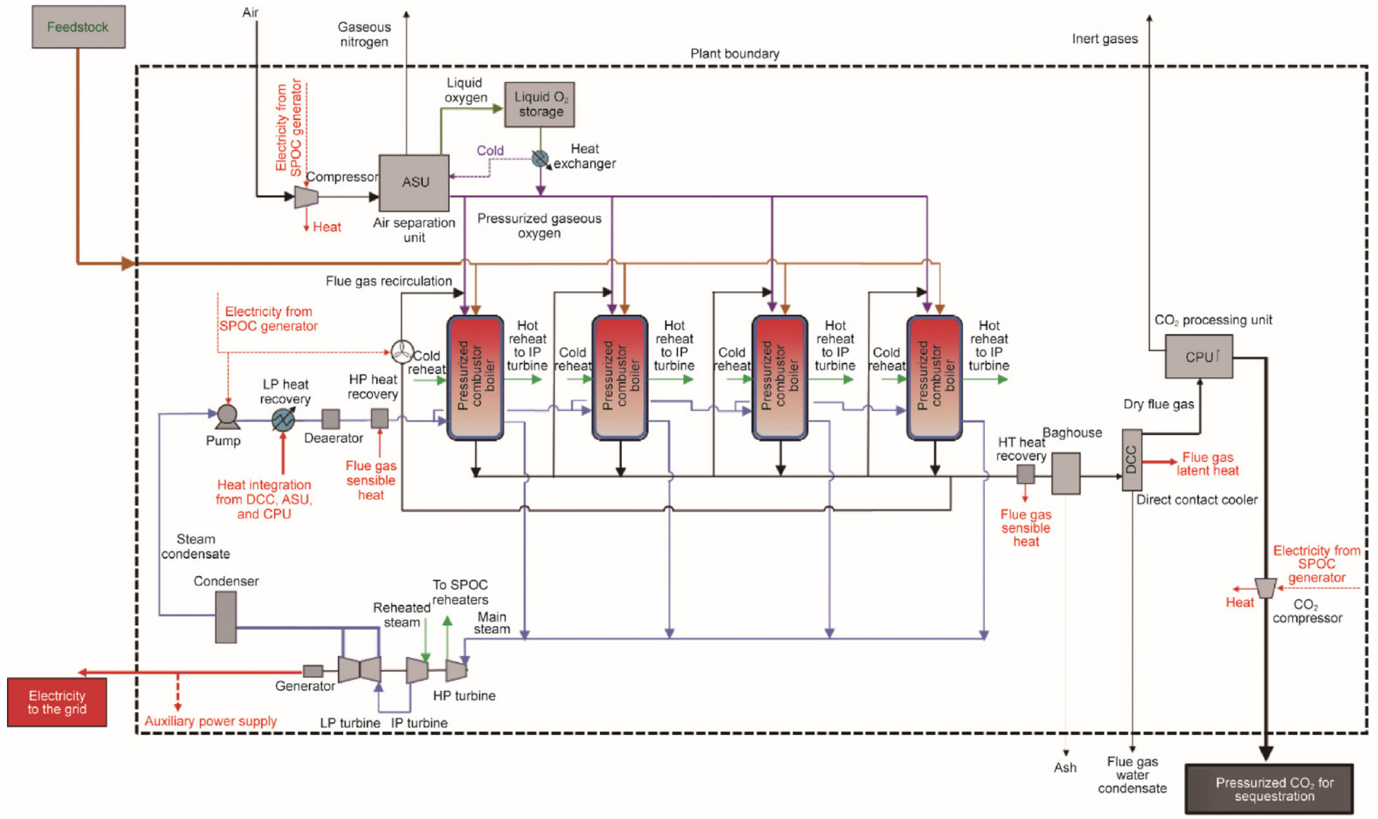

**Fig. 5.** Process flow diagram for modular SPOC process applied to a power generation retrofit. Note that only major elements on the steam side are represented.

**Table 1**
Comparison of HHV thermal efficiency of the SPOC process with atmospheric oxy and mainstream NETL baseline power plants with PCC.

| Process | CCS technology and capture (%) | Steam cycle | Fuel type | HHV thermal efficiency (%) |
|---|---|---|---|---|
| SPOC | SPOC, 95% | subC | 100% biomass | 32.1 |
| | | SC | 100% biomass | 34.9 |
| | | | 100% sub-bituminous coal | 34.8 |
| NETL baseline | | | | |
| S12F | Atmospheric oxy-combustion, 90% | SC | 100% sub-bituminous coal | 31.0 |
| S12B | Air-fired, amine-based PCC, 90% | SC | 100% sub-bituminous coal | 27.0 |
| B12B | Air-fired, amine-based PCC, 95% | SC[a] | 100% bituminous coal | 31.2 |
| PA1 | Air-fired, amine-based PCC, 90% | SC[a] | 20 wt% biomass | 30.8 |
| PA2 | Air-fired, amine-based PCC, 90% | SC[a] | 35 wt% biomass | 30.1 |
| PA3 | Air-fired, amine-based PCC, 90% | SC[a] | 49 wt% biomass | 29.2 |
| PA100 | Air-fired, amine-based PCC, 90% | SC[a] | 100 wt% biomass | 23.3 |

[a] The NETL baseline cases B12B, PA1, PA3, and PA100 use a more advanced turbine and higher grade coal along with higher moisture biomass as compared with the SPOC, S12F, and S12B cases [2,23,24].

used to heat the metal rolls that dry the paper to its final low moisture content. The steam, produced in an onsite industrial boiler (cogeneration plant), is supplied to the pulp drying and pulping processes at a temperature of 135 °C and a pressure of 3.1 bara.

In the example considered herein, the SPOC process is applied to an existing cogeneration plant to supply low-cost, carbon-negative steam and power to the paperboard plant, thus demonstrating the ability to meet the heat and power requirements of the paperboard plant while decarbonizing the industry. The SPOC process flow diagram for the cogeneration retrofit largely resembles that represented in Fig. 5, with the exception that the steam from the LP turbine is sent directly to the paperboard plant and the electricity from the generator is also used in the paperboard plant. Accordingly, Fig. 6 depicts a block flow diagram showcasing the main attributes of the cogeneration plant. PCC is chosen as a baseline for comparison. Both SPOC and PCC can be used as a retrofit to decarbonize the process, however, as will be shown, the SPOC process presents unique performance advantages as compared with PCC, particularly for cogeneration. Importantly, when retrofitting an older plant, the SPOC process enhances the net plant efficiency due to the high-efficiency SPOC boiler, while PCC has a significant efficiency penalty, particularly if using the original, less efficient boiler plus a dedicated boiler to meet the heat needs for PCC. If installing a new boiler that can meet the steam/power demands of the industrial process, PCC still needs additional heat for the regeneration in the PCC process and therefore a significantly larger boiler.

The SPOC cogeneration retrofit plant was designed to meet the needs of the recycled paperboard production plant. For this configuration, the gas-side process is identical to that shown in Fig. 5. For the steam side, a single reheat subC steam cycle (166 bara/566 °C/566 °C) is used with a steam turbine to generate

**Table 2**
Main parameters and assumptions of the process model of the SPOC retrofit plants.

| Item | Power/cogeneration |
|---|---|
| Fuel type | Sustainably sourced wood waste |
| HHV of biomass feedstock (kJ·kg$^{-1}$) | 17 664 |
| Type of Rankine cycle | SubC, single reheat |
| Steam conditions | 166 bara/566 °C/566 °C |
| Purity of oxygen product from ASU | 95.9 mol% |
| Oxygen in flue gas at the boiler outlet | 1 mol% |
| Isentropic efficiency of HP turbines | 83.7% |
| Isentropic efficiency of IP turbines | 88.7% |
| Isentropic efficiency of LP turbines | 92.5% |
| Heat loss of combustor and boiler | 1% of total thermal input |
| Electricity loss of generator | 1.5% |
| Capacity factor | 95% |
| $CO_2$ capture efficiency | 95% |
| $CO_2$ purity at the outlet of CPU | 99 mol% |
| Upstream $CO_2$ emissions (fuel transport and processing) relative to generated $CO_2$ within plant boundary (based on LCA) | 10% |

**Table 3**
Performance data of the SPOC retrofit plants.

| Item | Power | Cogeneration |
|---|---|---|
| Biomass feed rate (t·a$^{-1}$) | 340 802 | 536 112 |
| $CO_2$ generated (t·a$^{-1}$) | 588 230 | 923 304 |
| $CO_2$ net removal (t·a$^{-1}$) | 500 000 | 785 422 |
| Thermal input, HHV (MW$_{th}$) | 190.9 | 300.5 |
| Rankine cycle heat source (MW$_{th}$) | | |
| Heat to main steam | 143.1 | 221.7 |
| Heat to reheated steam | 26.0 | 40.0 |
| HP heat recovery | 5.1 | 7.7 |
| LP heat recovery (latent heat from DCC) | 16.7 | 30.2 |
| LP heat recovery (compressor waste heat from ASU + CPU) | 2.9 | 4.5 |
| Boiler efficiency (HHV) | 88% | 87% |
| Condenser duty (MW$_{th}$) | 111.9 | – |
| Gross power output (MW$_e$) | 82.6 | 86.4 |
| Auxiliaries (MW$_e$) | | |
| $CO_2$ capture/removal (ASU) | 14.6 | 23.0 |
| $CO_2$ compression | 2.8 | 4.4 |
| Ash handling | 0.02 | 0.03 |
| Processing the biomass | 0.1 | 0.2 |
| Boiler feed water pump | 1.5 | 2.3 |
| BOP | 2.4 | 3.7 |
| Total auxiliaries (MW$_e$) | 21.4 | 33.6 |
| Net output (MW-net) | 61.2 | 52.8 MW$_e$ + 217.1 MW$_{th}$ |
| HHV plant efficiency | 32.1% | 89.8% |

power, and steam from the LP turbine is used to supply heat/steam to the recycled paperboard plant. Heat rejection in the steam side of SPOC is almost completely avoided during cogeneration as the condenser and cooling tower are not needed. All the low-pressure steam (3.1 bara, 223 °C) from the LP turbine outlet is supplied to the pulp drying and pulping processes, which are the two most energy-intensive processes in the paperboard plant. Therefore, the net energy efficiency of a cogeneration SPOC plant can be very high, and the net electricity power output of SPOC can satisfy all the auxiliary load requirements of the cogeneration plant and partially meet the power demands in the paper production plant. It should be noted that there is assumed to be a 20% thermal loss due to steam distribution and returning condensates [26]. As a result, the steam temperature at the inlet of the paper production plants decreases to around 135 °C. As in a typical plant, steam condensation transfers heat to dry the pulp at nearly constant temperature, and the rest is directly mixed with the pulp in the pulping processes. The steam condensate (133 °C) from the pulp dryers returns to the SPOC plant, and the temperature decreases to around 50 °C due to transportation losses. Some makeup water is supplied at the inlet of the boiler feedwater pump to compensate for any losses of water in the steam cycle.

The recycled paperboard production plant considered in this study requires 173 MW$_{th}$ and 69 MW$_e$ to generate 500 000 t·a$^{-1}$ of recycled paperboard product. The Aspen Plus model used previously for the SPOC power plant [15] was adapted for a cogeneration plant with a total net energy output of ~270 MW (217.1 MW$_{th}$ and 52.8 MW$_e$). Considering steam distribution losses within the recycled paper plant (43 MW$_{th}$), the SPOC cogeneration is capable of supplying the required 38.3 MW$_{th}$ for pulping, pulp deinking, and refining, and 134.4 MW$_{th}$ for pulp drying (total of 173 MW$_{th}$). The SPOC turbine delivers a net 52.8 MW$_e$ to the recycled paperboard plant after all SPOC plant auxiliary loads are met (Table 3). This leaves a deficit of 16 MW$_e$ to be supplied to the recycled paperboard plant. While this additional electricity demand could be met by increasing the gross output of the turbine, it is assumed that the existing turbine is kept and that this additional power is purchased from the grid.

With a 95% carbon capture efficiency, the SPOC cogeneration plant is effectively removing 0.9 million tonnes of $CO_2$ from the atmosphere in a single year. In 2018, about 44 million tonnes of paper/paperboard were recycled [27], representing a total of 79 million tonnes $CO_2$e, showing the potential that SPOC presents to decarbonize this industry.

The SPOC cogeneration process was compared with a coal-fired subC power plant (B11B.95 NETL baseline) [23] coupled with state-of-the-art Shell Cansolv PCC with 95% capture efficiency. A detailed process descriptions of the PCC plant can be found in the NETL report for fossil energy plants [23]. The power supplied by the cogeneration plant with PCC is the same as that for the SPOC plant (216 MW$_{th}$ and 53 MW$_e$), but the total thermal input to the PCC plant is higher, 427 MW$_{th}$, due to the high thermal demand for solvent regeneration. This results in an efficiency for the PCC retrofit plant of only 63%. In contradistinction, the SPOC cogeneration plant achieves a total net energy efficiency of 89.8%, which is just 3 percentage points less than that of a similar cogeneration plant operating at the same net output but without carbon capture. The low efficiency of the PCC plant results in the need for 42% higher thermal input than the SPOC plant to generate the same total energy output.

## 4. Demonstration of biomass firing

Building on extensive (8+ years) experience with POC, biomass firing in the 125 kW$_{th}$ combustor was successfully demonstrated. The feedstock chosen was softwood biomass (40 mesh), which resembles the most common wood waste (e.g. sawmill residuals, wood product manufacturing residuals) in terms of composition and heating value (Table 4). The dry-feed system consists of a gravimetric screw feeder and a transfer vibratory table to allow for uniform and steady feeding to the burner. The dry-feed system, previously optimized for coal feeding, was modified to allow for feeding of either coal or biomass and was successfully tested. The oxygen concentration in the oxidizer stream was maintained at (31 ± 1) vol%, and the stoichiometric ratio was fixed at 1.1 to ensure that the excess oxygen at the exhaust was low (~2 vol%). Often it is necessary to have different burners for coal and biomass to ensure good flame stability for either fuel, particularly at the pilot scale. However, in this study the burner and combustor employed for biomass firing were identical to those used for coal firing to showcase the fuel flexibility of the SPOC process. At 15

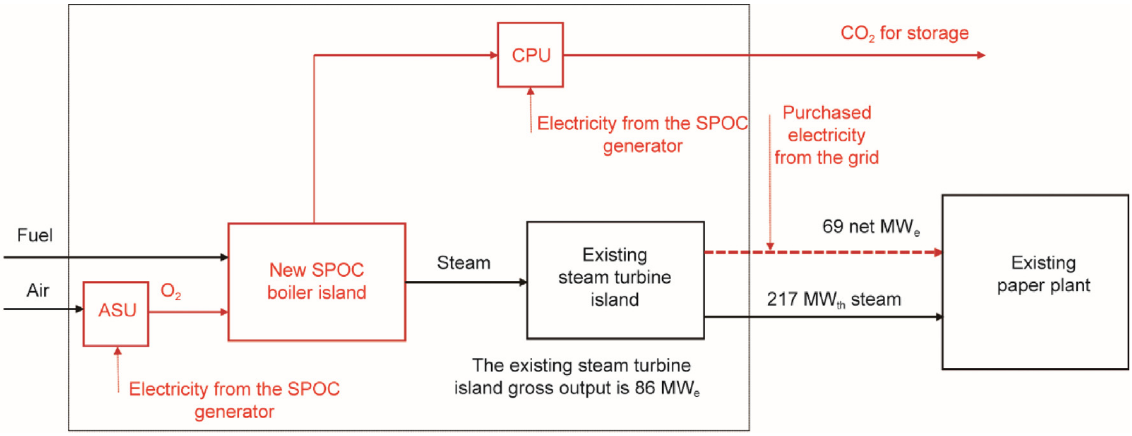

**Fig. 6.** Block flow diagram of the SPOC process for retrofitting an existing cogeneration plant to supply heat and power to an existing paper plant.

**Table 4**
Proximate and ultimate analyses and calorific content of the softwood biomass used in the pilot-scale tests.

| Item | As received (wt%) |
|---|---|
| Proximate analysis | |
| Moisture | 8.95 |
| Ash | 0.39 |
| Volatile matter | 79.54 |
| Fixed carbon[a] | 11.12 |
| Ultimate analysis | |
| Moisture | 8.95 |
| Carbon | 47.01 |
| Hydrogen | 5.51 |
| Nitrogen | 0.11 |
| Chlorine | < 0.01 |
| Sulfur | < 0.01 |
| Ash | 0.39 |
| Oxygen[a] | 38.03 |
| HHV ($kJ \cdot kg^{-1}$) | 20 024 |
| LHV ($kJ \cdot kg^{-1}$) | 18 608 |

[a] By difference.

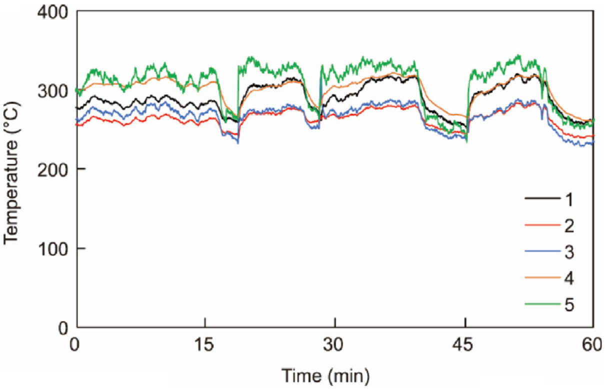

**Fig. 7.** Flame symmetry temperatures for an 80 $kW_{th}$ biomass flame over a steady-state 1 h period as measured by thermocouples #1–5.

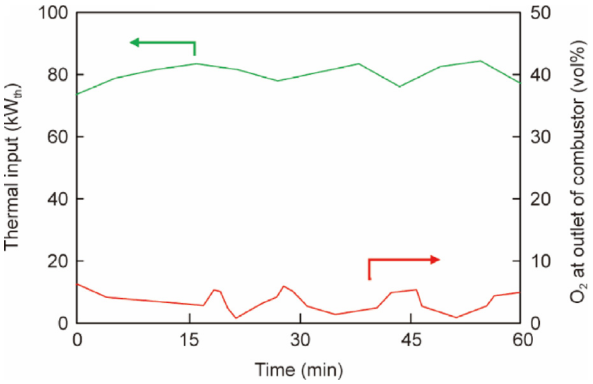

**Fig. 8.** Biomass thermal input ($kW_{th}$), and excess oxygen in the flue gas (vol%) for an 80 $kW_{th}$ biomass flame over a steady-state 1 h period.

bara pressure the oxidation and gasification reactions rates are greatly accelerated over atmospheric pressure conditions and this enhances flame stability.

The standard operating procedure (SOP) used for the biomass shakedown and testing was similar to the one already implemented for coal firing. The pressure vessel and biomass vessel were initially pressurized to 15 bara and the reactor was ignited using methane. Following a preheating period, fuel-switching from methane to biomass was initiated with a controlled ramping up of biomass and ramping down of methane. The system operation was very smooth and resembled prior runs of the facility using coal. After completion of fuel-switching over a period typically under 30 min, an 80 $kW_{th}$ biomass flame was stabilized. The continuous monitoring of the flame monitor signals, temperatures (flame symmetry and refractory wall), differential pressure, and outlet gas composition ($O_2$, $CO_2$, and CO) showed that the system was stable and steady throughout the 100% biomass firing. Fast fuel-switching in under 10 min was also successfully achieved. Upon reaching pure biomass conditions, the facility was operated in steady-state for a period of 1–2 h, during which time flue gas sampling was performed.

During this steady-state period, the flame showed excellent symmetry as shown in Fig. 7. Measurements of flue gas composition downstream of the combustor indicated that the excess oxygen at the outlet was low (2–3 vol%; Fig. 8), and the CO was also low, under 250 ppm. The flue gas was also sampled using an isokinetic oil-cooled sampling probe inserted through the bottom of the reactor (upstream of the DCC). All lines are heat-traced and temperature-controlled to prevent loss of condensable species. The sampled flue gas flows through a high-pressure, high-temperature filter to collect particulate matter (ash/char) for further analysis. Downstream of the filter, the flue gas has two possible paths: ① directly into a high-pressure gas cell coupled to an FTIR gas analyzer, or ② through a pressure-reducing valve and

**Table 5**
Major pollutants and particle burnout measured in steady state conditions during oxy-firing with biomass when sampling at the combustor outlet (upstream of the DCC).

| Major pollutants (dry basis) | Value | Unit |
|---|---|---|
| $CO_2$ | 97 | vol% |
| CO | 250 | ppm |
| $O_2$ | 2–3 | vol% |
| $NO_x$ | 40 | ppm |
| $SO_2$ | ~0 | ppm |
| HCl | < 5 | ppm |
| Particle burnout | 99.9 | % |

then into an atmospheric pressure Testo 350 gas analyzer. The latter is used to measure stable species and the former potentially unstable species. Fly ash was collected using a total collection filter and, due to its very limited amount, analyzed for carbon content in the ash using thermogravimetric analysis (TGA) and total organic content (TOC) analysis. For both methods a burnout of 99.9% was measured. The $NO_x$ concentration was ~40 ppm and the $SO_2$ concentration was zero when sampling at the outlet of the combustor before the DCC (Table 5). The ultra-low concentration of $SO_2$ was expected due to the absence of sulfur in the biomass feedstock used. The low $NO_x$ measured is consistent with prior results for coal firing under POC conditions. The high-pressure and oxy-combustion conditions result in higher partial pressure of $CO_2$ and enhance char gasification reactions that produce reducing gases such as CO that improve $NO_x$ reduction. Based on the FTIR results, the HCl concentration in the biomass flue gas was below 5 ppm, which is the detection limit of the FTIR signal. It should be noted that the entire sampling line was temperature-controlled (> 200 °C) to avoid any HCl loss.

## 5. Conclusions

The SPOC process leverages pressure and fuel-staging to generate reliable, low-cost, low-carbon or carbon-negative heat and/or power and has been proven to be ideally suited for combined heat and power applications. The technology relies on proven principles as opposed to high-risk concepts and minimizes the efficiency penalty to only 3.8 percentage points from that of an unabated coal-fired power plant. The SPOC biomass plant yields considerably higher efficiency than a PCC-equipped plant, whether for power or cogeneration while removing $CO_2$ from the atmosphere. Particularly for a power generation retrofit application, the subC SPOC biomass power plant can reach a thermal efficiency of 32.1% (HHV), or 36% for a SC cycle using an advanced turbine. This is 8–9 percentage points higher than the equivalent SC plant equipped with PCC using the same biomass feedstock, representing 33% more energy extracted from the same biomass fuel. The SPOC cogeneration retrofit plant achieves a total net energy efficiency of 89.8%, while a plant retrofitted with PCC would require 42% higher thermal input to generate the same total energy output.

Following improvements to the dry-feed system, the pilot-scale facility at WashU is now compatible with both coal and biomass and requires no changes to utilize either fuel. Importantly, pressurized biomass oxy-combustion was demonstrated for the first time at the 80 $kW_{th}$ scale. The biomass combustor showed excellent performance during startup, steady-state, and turndown when firing 100% biomass without support of a gaseous pilot flame, and with low excess oxygen in the flue gas (< 2 vol%). A pressurized Nafion dryer coupled to a FTIR analyzer for measuring online flue gas composition at pressure were successfully applied to biomass firing for the first time.

## CRediT authorship contribution statement

**Duarte Magalhaes:** Writing – original draft, Visualization, Validation, Methodology, Investigation, Formal analysis, Data curation, Conceptualization. **Mao Cheng:** Writing – review & editing, Validation, Methodology, Investigation, Formal analysis, Data curation, Conceptualization. **Zachariah Wargel:** Methodology, Investigation. **Richard L. Axelbaum:** Writing – review & editing, Supervision, Resources, Project administration, Conceptualization.

## Declaration of competing interest

The authors declare that they have no known competing financial interests or personal relationships that could have appeared to influence the work reported in this paper.

## Acknowledgments

The authors greatly appreciate Mr. Scott Hume's insightful advice and input that greatly improved the process modeling of SPOC. This work was supported by the United States Department of Energy (DE-FE0031925 and DE-FE0032515).

## References

[1] Shehabi A, Smith SJ, Hubbard A, Newkirk A, Lei N, Siddik MAB, et al. United States data center energy usage report. Report. Berkeley: Lawrence Berkeley National Laboratory; 2024. Contract No.: LBNL-2001637.
[2] Matuszewski M. Cost and performance for low-rank pulverized coal oxycombustion energy plants. Report. Albany: National Energy Technology Laboratory; 2010.
[3] Gopan A, Verma P, Yang Z, Axelbaum RL. Quantitative analysis of the impact of flue gas recirculation on the efficiency of oxy-coal power plants. Int J Greenh Gas Control 2020;95:102936.
[4] Axelbaum R, Kumfer B, Gopan A, Yang Z, Phillips J, Pint B. Staged, high pressure oxy-combustion technology: development and scale-up. Report. Washington, DC: United Stated Department of Energy; 2017.
[5] Xia F, Yang Z, Adeosun A, Gopan A, Kumfer BM, Axelbaum RL. Pressurized oxy-combustion with low flue gas recycle: computational fluid dynamic simulations of radiant boilers. Fuel 2016;181:1170–8.
[6] Li L, Akkerman V, Magalhaes D, Yang Z, Axelbaum RL. Investigation of thermal radiation under pressurized oxy-combustion conditions. Int J Energy Clean Environ 2024;25(8):41–51.
[7] Li L, Akkerman V, Yang Z, Magalhaes D, Axelbaum RL. Computational analysis of the impact of boundary conditions on a particle-laden flow: a case study in a pressurized oxy-coal combustor. Int J Energy Clean Environ 2023;24(8):191–203.
[8] Li X, Lin H, Wang G, Dai G, Chen YQ, Luo Y, et al. A full-scale staged, pressurized oxy-biomass combustion towards BECCS: performance assessment via CFD approach. Energy 2025;326:136262.
[9] Montero AI. Towards large Eddy simulation of a staged, pressurized oxy-fuel [dissertation]. Morgantown: West Virginia University; 2020.
[10] Gopan A. Studies in pressurized oxy-combustion: process development and control of radiative heat transfer [dissertation]. St. Louis: Washington University in St. Louis; 2017.
[11] Yang Z, Khatri D, Verma P, Li T, Adeosun A, Kumfer BM, et al. Experimental study and demonstration of pilot-scale, dry feed, oxy-coal combustion under pressure. Appl Energy 2021;285:116367.
[12] Verma P, Yang Z, Axelbaum RL. A direct contact cooler design for simultaneously recovering latent heat and capturing $SO_x$ and $NO_x$ from pressurized flue gas. Energ Conver Manage 2022;254:115216.
[13] Stokie D, Verma P, Kumfer BM, Yablonsky G, Suresh AK, Axelbaum RL. Pilot-scale testing of direct contact cooler for the removal of $SO_x$ and $NO_x$ from the flue gas of pressurized oxy-coal combustion. Chem Eng J 2021;414:128757.
[14] ur Rahman Z, Wang X, Zhang J, Yang Z, Dai G, Verma P, et al. Nitrogen evolution, $NO_X$ formation and reduction in pressurized oxy coal combustion. Renew Sustain Energy Rev 2022;157:112020.
[15] Hume S. Enabling staged pressurized oxy-combustion: improving flexibility and performance at reduced cost. Report. Palo Alto: Electric Power Research Institute (EPRI); 2019.
[16] Hagi H, Nemer M, Le Moullec Y, Bouallou C. Towards second generation oxy-pulverized coal power plants: energy penalty reduction potential of pressurized oxy-combustion systems. Energy Procedia 2014;63:431–9.
[17] Hu F, Sun H, Zhang T, Wang Q, Li Y, Liao H, et al. Comparative study on process simulation and performance analysis in two pressurized oxy-fuel combustion power plants for carbon capture. Energ Conver Manage 2024;303:118178.

[18] Cheng M, Wargel Z, Magalhaes D, Axelbaum R. A novel optical instrument for on-line measurement of particle size distribution—application to clean coal technologies. Energies 2025;18(3):1–12.

[19] Yang W, Zhu Y, Cheng W, Sang H, Yang H, Chen H. Characteristics of particulate matter emitted from agricultural biomass combustion. Energy Fuels 2017;31(7):7493–501.

[20] Cheng M, Verma P, Yang Z, Axelbaum RL. Flexible cryogenic air separation unit—an application for low-carbon fossil-fuel plants. Separ Purif Tech 2022;302:122086.

[21] Gopan A, Kumfer BM, Phillips J, Thimsen D, Smith R, Axelbaum RL. Process design and performance analysis of a staged, pressurized oxy-combustion (SPOC) power plant for carbon capture. Appl Energy 2014;125:179–88.

[22] Skone TJ, James RE, Jamieson M, Cooney G, Schivley G, Shih CY. Upstream dashboard version 3. Report. Albany: National Energy Technology Laboratory; 2016.

[23] Schmitt T, Leptinsky S, Turner M, Zoelle A, Woods M, Shultz T, et al. Cost and performance baseline for fossil energy plants. Volume 1: bituminous coal and natural gas to electricity. Report. Albany: National Energy Technology Laboratory; 2022.

[24] James B. Cost and performance baseline for fossil energy plants. Volume 3B: low rank coal to electricity: combustion cases. Report. Albany: National Energy Technology Laboratory; 2011.

[25] Tufano L. WestRock agrees to buy paper recycler, renewable energy company for $289M. Report. Newton: Wastedive; 2015.

[26] Brueske S, Sabouni R, Zach C, Andres H. US manufacturing energy use and greenhouse gas emissions analysis. Report. Oak Ridge: Oak Ridge National Lab (ORNL); 2012.

[27] Paper and paperboard: material-specific data. Report. Washington, DC: United States Environmental Protection Agency; 2022.